Anomalous Nernst Effect of Fe_3O_4 Single Crystal

R. Ramos[*,1], M.H. Aguirre[1,2], A. Anadón[1,2], J. Blasco[2,3], I. Lucas[1,4], K. Uchida[5,6], P.A. Algarabel[2,3], L. Morellón[1,2], E. Saitoh[5,7,8,9] and M.R. Ibarra[1,2]

[1] *Instituto de Nanociencia de Aragón, Universidad de Zaragoza, E-50018 Zaragoza, Spain*

[2] *Departamento de Física de la Materia Condensada, Universidad de Zaragoza, E-50009 Zaragoza, Spain*

[3] *Instituto de Ciencia de Materiales de Aragón, Universidad de Zaragoza and Consejo Superior de Investigaciones Científicas, 50009 Zaragoza, Spain*

[4] *Fundación ARAID, 50018 Zaragoza, Spain*

[5] *Institute for Materials Research, Tohoku University, Sendai 980-8577, Japan*

[6] *PRESTO, Japan Science and Technology Agency, Saitama 332-0012, Japan*

[7] *WPI Advanced Institute for Materials Research, Tohoku University, Sendai 980-8577, Japan*

[8] *Advanced Science Research Center, Japan Atomic Energy Agency, Tokai 319-1195, Japan and*

[9] *CREST, Japan Science and Technology Agency, Sanbancho, Tokyo 102-0075, Japan*

(Dated: July 29, 2015)

[*)] Electronic mail: ramosr@unizar.es

Abstract

We report a complete characterization of the anomalous Nernst effect (ANE) and its relationship with the anomalous Hall effect (AHE) in Fe_3O_4. By combining full thermoelectric and electric transport measurements as a function of temperature, we have verified that the universal scaling relation between the anomalous Hall and diagonal conductivities ($\sigma_{zy} \propto \sigma_{zz}^{1.6}$), observed in materials with bad-metal-hopping type of conduction, is also applicable to the thermoelectric transport. We further show that the ANE and AHE are commonly related through the Mott relation, therefore demonstrating its validity for anomalous transport phenomena in materials with conduction in the the dirty regime.

PACS numbers: 75.47.-m, 75.47.Lx, 72.20.Pa, 71.30.+h

Thermoelectric power conversion is a promising approach for environmental friendly energy generation. Traditionally it has exploited the generation of an electric voltage by a thermal gradient, the Seebeck effect. However the efficiency of conventional thermoelectric materials is limited by their ability to sustain a thermal gradient, one approach is focused on the reduction of the thermal conductivity but the electronic carrier contribution represents an obstacle for the efficiency of thermoelectric devices, since it presents a lower limit to the minimum thermal conductivity that can be attained. Contrary to this the electronic conductivity has to be maximized. The recent discovery of the spin Seebeck effect (SSE)[1] and its observation in magnetic insulators[2] offers a possible route to overcome this limitation and the possibility of exploiting magnetic oxide materials, which are not generally suitable for conventional thermoelectric generation, due to the absence of mobile carriers. This discovery expanded the field of spin caloritronics[3], which is focused on the study of the correlation between heat, spin and charge currents in magnetic materials. This area has the potential for heat manipulation[4] and thermoelectric power generation exploiting other thermomagnetic effects in magnetic materials, as it has been recently shown with the observation of an increased voltage in SSE[5] and anomalous Nernst effect (ANE) thermopile structures.[6]

In light of the above, thermomagnetic properties of magnetic oxides are key issues to establish a landscape of suitable materials for heat induced generation of spin currents, therefore studying mechanisms that can affect the spin Seebeck effect is of utter importance in order to deepen our knowledge on the spin-heat interaction. This has been recently shown in studies on SSE and ANE,[7–11] where the relevance of ANE to spin caloritronics has been investigated. Phenomenologically, the anomalous Nernst effect consists on the generation of an electric field ($\vec{E}_{ANE}$) in the direction parallel to the outer product of the magnetization of the sample ($\vec{M}$) and applied thermal gradient (∇T) (see Fig. 1(a)) and can be expressed as:

$$\vec{E}_{ANE} = -Q_S \mu_0 (\vec{M} \times \nabla T), \tag{1}$$

where μ_0 and Q_S are the vacuum permeability and ANE coefficient, respectively. The physical origin of the ANE is still to be clarified, since the number of studies on this effect is scarce[6,12–14] and never reported in magnetite.

Here, we report the experimental measurement of ANE in Fe_3O_4 single crystal. Magnetite is a well known material which presents a high Curie temperature (858 K) and an expected half metallic behavior, these properties have made it a potential candidate for spintronic

applications,[15] inspiring a number of investigations on thin films and heterostructures.[16–18] Magnetite is also known to present a metal to insulator transition at a temperature of around 125 K, known as the Verwey transition, whose mechanism has been the matter of controversy for decades.[19,20] Despite being the oldest magnetic material known to mankind, the ANE in magnetite has remained elusive and there are not available reports to date. Furthermore recent observation of the spin Seebeck effect in magnetite thin films[21] points to the need to investigate the fundamental thermomagnetic transport properties of this material. This study will help in the advancement of heat-spin interaction knowledge and possibly a better control of heat driven spin currents, unveiling the role of conduction on the ANE of this highly correlated oxide.

Two $Fe_3O_4(001)$ single crystals were used for this study to confirm the reproducibility of the results (labelled S1 and S2). They were obtained by the floating zone method,[22] showing a saturation magnetization at 5 K of 4.11 μ_B, and the Verwey transition temperature (T_V) at 123.5 K with a narrow transition width ($\Delta T = 1$ K), these features correspond to highly stoichiometric samples.[23,24] Further details of sample preparation and properties can be obtained elsewhere.[23,25,26]

Anomalous Nernst effect measurements were performed in a home made thermoelectric measurements probe compatible with an Oxford spectrostat NMR40 continuous flow He cryostat. The sample is placed between two Cu plates; a resistive heater is connected to the upper Cu plate and the lower Cu plate provides the heat sink and is in direct contact with the thermal link of the cryostat. A temperature gradient is generated by application of an electric current to the heater and the temperature difference between upper and lower plate is monitored by two T-type thermocouples. To avoid electrical contact of the Cu plates with the sample, two sapphire single crystals were placed between the top/bottom of the sample and the top/bottom Cu plate, this ensures electrical insulation without disruption of the thermal contact. The samples were contacted with thin Al wires with the diameter of 25 μm. To minimize thermal losses, the temperature of the wires is stabilized by thermal anchoring to the sample holder. The thermoelectric voltage in Fe_3O_4 was monitored with a Keithley 2182A nanovoltmeter.

The dimensions of the samples used for the ANE measurements were $L_x = 1$ mm, $L_y = 4$ mm and $L_z = 1$ mm. The distance between the voltage probing contacts was $L_c = 2$ mm. A thermal gradient was applied in the z direction, while a sweeping magnetic field

parallel to the x direction is applied while the generated voltage is measured in the y direction (see Figure 1(a) for the measurement geometry). Small misalignments when centering the sample with respect to the upper plate can generate spurious in-plane gradients which can give a contribution from the magnetothermopower. This contribution was removed by antisymmetrization of the measured voltage.

Figure 1(b) shows the results observed in the Fe_3O_4 single crystal for the magnetic field dependence of the thermally induced transversal voltage (V_y) measured at room temperature when the magnetic field is applied parallel to the x direction, for different magnitudes of applied thermal gradient between the top and bottom of the sample. We can clearly see that the magnitude of the voltage increases with the magnitude of the temperature difference (ΔT), the inset shows the magnitude of the measured voltage at saturation ($V_y^{sat} = V_y(0.7$ T)) versus ΔT, where the expected linear dependence is observed. The anomalous Nernst signal can be extracted from the slope of this curve and geometrically correcting for the measurement geometry ($S_{zy} = (V_y^{sat}/\Delta T)(L_z/L_c)$). Obtaining the following values at room temperature; $S_{zy} = 0.122 \pm 0.003$ μV/K and $Q_S = \frac{S_{zy}}{\mu_0 M_S} = 0.189 \pm 0.004$ μV/KT, where M_S is the magnetization saturation. These values are similar for both samples within experimental error. It is important to remark that the contribution from the normal Nernst effect (NE) to the observed signal does not affect the measured ANE values. We estimated the NE obtained from the slope of V_y vs $\mu_0 H$ for fields larger than 0.5 T at different thermal gradients, obtaining a coefficient of 0.01 μV/KT. This gives a contribution from the NE to the ANE signal of only 7 nV/K at 0.7 T, which is of the same order of magnitude of the estimated error for S_{zy}. This behavior is consistently observed at all temperatures. Furthermore, the anomalous Nernst effect signal is expected to closely follow the magnetization of the sample (see Eq.(1)). This can be observed in Figure 1(c), where it is depicted the transversal thermoelectric voltage (V_y) compared to the magnetization measured at 300 K with a vibrating sample magnetometer.

The angular dependence of V_y was measured by changing the direction of the applied magnetic field as shown in Figure 2(a). Figure 2(b) shows the hysteresis loops for the thermally induced transversal voltage (V_y) measured at different orientations of magnetic field. The measured voltage at saturation (V_y^{sat}) behaves as expected with a sinusoidal dependence and maximum signal when the magnetic field, the applied thermal gradient and the direction of the measurement of voltage are at right angles to one another (see Fig. 2(c)) , confirming

the agreement with the phenomenological equation of the anomalous Nernst effect (Eq. (1)). The temperature dependence of the observed ANE measured in both samples is shown in Figure 3(a). It can be observed that the ANE shows a weak dependence with the temperature down to temperatures just above T_V. At the Verwey transition temperature the magnitude of S_{zy} abruptly changes, showing a sign reversal and an increased magnitude. As the temperature is further reduced the signal recovers its high temperature sign and shows an increased magnitude in comparison to what it is observed above T_V.

In order to analyse the data we need to consider the expression from the electron transport theory $J_i = \sigma_{ij}E_j - \alpha_{ik}\nabla_k T$, where J_i stands for the electron current, E_j is the electric field and $\nabla_k T$ is the applied thermal gradient, the coefficients σ_{ij} and α_{ik} are the elements of the electrical and thermoelectric conductivity tensors, respectively. Under open circuit conditions ($J_y = 0$), we obtain the following expression for the ANE electric field; $E_y = \rho[\alpha_{zy} - \alpha_{zz}\frac{\sigma_{zy}}{\sigma_{zz}}]\nabla_z T$ (where $\rho = \rho_{zz}$ is the resistivity of the sample), this can be expressed in terms of the Seebeck coefficient $S = \rho\alpha_{zz}$ and the Hall angle $tan\theta_{zy} = \sigma_{zy}/\sigma_{zz}$ as

$$E_y = [\rho\alpha_{zy} - Stan\theta_{zy}]\nabla_z T. \tag{2}$$

In this equation the first term arises from the non-diagonal component of the thermoelectric conductivity tensor and the second term from the non-diagonal component of the electrical conductivity tensor. Therefore in order to evaluate the origin of the observed transversal voltage (V_y), it is necessary to perform resistivity, Seebeck and anomalous Hall effect (AHE) measurements. Figure 3(b) shows the Seebeck effect obtained for a Fe_3O_4 single crystal with the thermal gradient applied in the same direction as in the ANE measurement and the resistivity data as a function of temperature. The Seebeck coefficient is approximately constant above the Verwey transition, with a value of $\sim$ - 50 μV/K. At $T < T_V$ it shows a strong enhancement in magnitude, in agreement with previous reports.[27,28] AHE measurements were performed using van der Pauw technique in disc shaped magnetite single crystals from the same batch as those used for the thermoelectric measurements. The samples used for AHE have a diameter $d = 4$ mm and a thickness $t = 0.8$ mm. The results are shown in figure 3(c), obtaining a scaling relation $\sigma_{zy} = -10^{-3.9\pm0.1}\sigma_{zz}^{1.53\pm0.06}$ (see inset of Fig.3(c)), these results are in agreement with the universal scaling of the AHE in Fe_3O_4.[29–31] Considering this relation and the expression for $tan\theta_{zy} = \sigma_{zy}/\sigma_{zz}$, we obtained $tan\theta_{zy} = -10^{-3.9\pm0.1}\sigma_{zz}^{0.53\pm0.06}$. Using the expression for the Hall angle and the measured Seebeck effect we can estimate the

contribution from the non-diagonal component of the electrical conductivity to the observed anomalous Nernst signal.

Since both samples show similar behavior, we will focus our analysis on sample S1. Figure 4 shows the comparison between the observed anomalous Nernst signal and the joint contribution of the Seebeck effect and the non-diagonal component of the conductivity tensor (AHE) for $T > 110$ K , we can observe that the magnitude of $Stan\theta_{zy}$ is smaller than that of the observed signal. From this quantities we can extract the non-diagonal component of the thermoelectric tensor ($\alpha_{zy} = \frac{1}{\rho}(\frac{E_y}{\nabla T} + Stan\theta_{zy})$), this term gives information about the transversal current which is generated upon application of a thermal gradient and by Onsager reciprocity it is also possible to know the amount of transverse heat current generated by an electric field ($J_y^Q = \tilde{\alpha}_{zy}E_z$, since $\tilde{\alpha}_{zy} = \alpha_{zy}T$).[32]

The inset of Figure 4 shows the temperature dependence of S_{zy} for the full temperature range. At T_V magnetite undergoes an abrupt change of crystallographic structure from cubic to monoclinic symmetry,[33] this is accompanied by further anomalies in a series of related parameters that affect the magnetic, thermodynamic and electrical properties of the solid.[19] For instance, the Seebeck effect shows an enhancement and anisotropic behavior which depends on the direction of the applied thermal gradient with respect to the crystallographic axes.[28] Furthermore the magnetoresistance (MR) and magnetoseebeck of Fe_3O_4 present a sharp peak at T_V and are strongly enhanced in the vicinity of $T < T_V$.[34] This complex behavior of several inter-related parameters in the insulating phase complicates the interpretation of the observed results and points to the need of further studies to clarify the origin of the observed signal below T_V. Therefore we will concentrate our analysis on the results obtained in the cubic phase of magnetite, above the Verwey transition.

For our analysis we will consider the Mott expression, which relates the off-diagonal component of the thermoelectric conductivity tensor α_{zy} to the derivative of σ_{zy} at the chemical potential:

$$\alpha_{zy} = (\frac{\pi^2 k_B^2}{3e})T\frac{d}{d\epsilon}[\sigma_{zy}(\epsilon)]_\mu \tag{3}$$

where k_B is the Boltzmann constant, e the electron charge and μ the chemical potential. If we consider the power law for the anomalous Hall effect, $\rho_{zy} = \lambda\rho_{zz}^n$ and substitute it in the Mott relation described above.[35] We obtain the following expressions for the anomalous

Nernst response (see appendix):

$$S_{zy} = \rho^{(n-1)}[\frac{\pi^2 k_B^2}{3e} T\lambda' - (n-1)\lambda S] \tag{4}$$

and

$$\alpha_{zy} = \rho^{(n-2)}[\frac{\pi^2 k_B^2}{3e} T\lambda' - (n-2)\lambda S] \tag{5}$$

where λ' is the energy derivative of the prefactor in the power law. In Figures 5(a) and 5(b) we can observe the fitting of S_{zy} and α_{zy} to the above obtained equations (where the fitting parameters are λ', λ and n), with the values for λ and n in agreement to the ones previously extracted by AHE in magnetite.[29,30] It is interesting to observe that the equations can describe the behavior of the ANE in the cubic phase and that the obtained value of $n \sim 0.4$ is in agreement with the universal scaling for materials with bad-metal-hopping conduction regime,[36] as previously measured by the anomalous Hall effect in magnetite ($\sigma_{zy} \propto \sigma_{zz}^{\alpha}$, where $\alpha = 1.6$, since $\sigma_{zy} = \rho_{zy}/\rho_{zz}^2$ and $\alpha = 2 - n$). Therefore proving the validity of the Mott relation in the electrically conductive phase and confirming the universal scaling by means of thermoelectric measurements.

In conclusion, we have measured the previously elusive anomalous Nernst effect in bulk magnetite. We have further proved the validity of the Mott relation for the off-diagonal transport coefficients in the cubic phase and demonstrated that the universal scaling between the anomalous Hall and diagonal conductivity is also applicable for the thermoelectric transport phenomena. This result is relevant to advance in the knowledge of the anomalous transport in materials with electronic conduction in the bad-metal-hopping regime.

The authors thank S. Maekawa and T. Kikkawa for valuable discussions. This work was supported by the Spanish Ministry of Science (trough projects PRI-PIBJP-2011-0794, MAT2011-27553-C02, including FEDER funding), the Aragón Regional Government (project E26) and Thermo-Spintronic Marie Curie CIG (Grant agreement: 304043). This research was also supported by Strategic International Cooperative Program, Japan Science and Technology Agency (JST), PRESTO-JST "Phase Interfaces for Highly Efficient Energy Utilization", CREST-JST "Creation of Nanosystems with Novel Functions through Process Integration", a Grant-in-Aid for Young Scientists (A) (25707029) from MEXT, Japan, a Grant-in-Aid for Scientific Research (A) (24244051) from MEXT, Japan, LC-IMR of Tohoku University, the Tanikawa Fund Promotion of Thermal Technology, and Casio Science

Promotion Foundation.

Appendix: Derivation of the equations for the anomalous Nernst response

Here we proceed to describe the detailed derivation of equations 4 and 5 of the text, obtained from the Mott relation for the anomalous transport. We start considering the equation for the anomalous Nernst signal:

$$S_{zy} = \frac{E_y}{\nabla_z T} = \rho\alpha_{zy} - Stan\theta_{zy} \tag{A.1}$$

where ρ, α_{zy} are the resistivity, off-diagonal component of thermoelectric conductivity and $S = \frac{\alpha_{zz}}{\sigma}$ and $tan\theta_{zy} = \frac{\sigma_{zy}}{\sigma}$ are the Seebeck coefficient and Hall angle respectively.
The Mott expression for the anomalous transport relates the off-diagonal components of the thermoelectric and electric conductivities and is given by:

$$\alpha_{zy} = (\frac{\pi^2 k_B^2}{3e})T\frac{d}{d\epsilon}[\sigma_{zy}(\epsilon)]_\mu \tag{A.2}$$

Now we proceed to calculate the energy derivative of of σ_{zy}, considering the expression for the scaling of the anomalous Hall effect; $\rho_{zy} = \lambda\rho^n$ (where $\sigma_{zy} = \frac{\rho_{zy}}{\rho_{zz}^2+\rho_{zy}^2} \simeq \frac{\rho_{zy}}{\rho^2}$), which is equivalent to $\sigma_{zy} = \lambda\sigma^{2-n}$, we obtain:

$$\frac{\partial}{\partial\epsilon}(\sigma_{zy})_\mu = (\frac{\partial\lambda}{\partial\epsilon})_\mu\sigma^{(2-n)} + \lambda(2-n)\sigma^{(1-n)}(\frac{\partial\sigma}{\partial\epsilon})_\mu \tag{A.3}$$

introducing this relation into equation (A.2) and considering the Mott expression for the Seebeck effect ($S = \frac{\pi^2 k_B^2}{3e}T\frac{\partial}{\partial\epsilon}(ln\sigma)_\mu$), we can simplify to:

$$\alpha_{zy} = \rho^{(n-2)}[\frac{\pi^2 k_B^2}{3e}T\lambda' - (n-2)\lambda S] \tag{A.4}$$

where $\lambda' = (\frac{\partial\lambda}{\partial\epsilon})_\mu$ and $\rho = 1/\sigma$, inserting this expression into equation (A.1) for the anomalous Nernst signal, we obtain:

$$S_{zy} = \rho^{(n-1)}[\frac{\pi^2 k_B^2}{3e}T\lambda' - (n-1)\lambda S] \tag{A.5}$$

---

[1] K. Uchida, S. Takahashi, K. Harii, J. Ieda, W. Koshibae, K. Ando, S. Maekawa, and E. Saitoh, Nature **455**, 778 (2008).

[2] K. Uchida, J. Xiao, H. Adachi, J. Ohe, S. Takahashi, J. Ieda, T. Ota, Y. Kajiwara, H. Umezawa, H. Kawai, et al., Nat. Mater. **9**, 894 (2010).

[3] G. E. W. Bauer, E. Saitoh, and B. J. van Wees, Nat. Mater. **11**, 391 (2012).

[4] T. An, V. I. Vasyuchka, K. Uchida, A. V. Chumak, K. Yamaguchi, K. Harii, J. Ohe, M. B. Jungfleisch, Y. Kajiwara, H. Adachi, et al., Nat. Mater. **12**, 549 (2013).

[5] K. Uchida, T. Nonaka, T. Yoshino, T. Kikkawa, D. Kikuchi, and E. Saitoh, Appl. Phys. Express **5**, 093001 (2012).

[6] Y. Sakuraba, K. Hasegawa, M. Mizuguchi, T. Kubota, S. Mizukami, T. Miyazaki, and K. Takanashi, Appl. Phys. Express **6**, 033003 (2013).

[7] S. Y. Huang, X. Fan, D. Qu, Y. P. Chen, W. G. Wang, J. Wu, T. Y. Chen, J. Q. Xiao, and C. L. Chien, Phys. Rev. Lett. **109**, 107204 (2012).

[8] S. Bosu, Y. Sakuraba, K. Uchida, K. Saito, W. Kobayashi, E. Saitoh, and K. Takanashi, J. Appl. Phys. **111**, 07B106 (2012).

[9] M. Weiler, M. Althammer, F. D. Czeschka, H. Huebl, M. S. Wagner, M. Opel, I.-M. Imort, G. Reiss, A. Thomas, R. Gross, et al., Phys. Rev. Lett. **108**, 106602 (2012).

[10] T. Kikkawa, K. Uchida, S. Daimon, Y. Shiomi, H. Adachi, Z. Qiu, D. Hou, X.-F. Jin, S. Maekawa, and E. Saitoh, Phys. Rev. B **88**, 214403 (2013).

[11] T. Kikkawa, K. Uchida, Y. Shiomi, Z. Qiu, D. Hou, D. Tian, H. Nakayama, X.-F. Jin, and E. Saitoh, Phys. Rev. Lett. **110**, 067207 (2013).

[12] W. Nernst, Ann. Phys. **267**, 760 (1887).

[13] T. Miyasato, N. Abe, T. Fujii, A. Asamitsu, S. Onoda, Y. Onose, N. Nagaosa, and Y. Tokura, Phys. Rev. Lett. **99**, 086602 (2007).

[14] M. Mizuguchi, S. Ohata, K. Uchida, E. Saitoh, and K. Takanashi, Appl. Phys. Express **5**, 093002 (2012).

[15] J. Sinova and I. Zutic, Nat. Mater. **11**, 368 (2012).

[16] R. Ramos, S. K. Arora, and I. V. Shvets, Phys. Rev. B **78**, 214402 (2008).

[17] H.-C. Wu, M. Abid, B. S. Chun, R. Ramos, O. N. Mryasov, and I. V. Shvets, Nano Lett. **10**, 1132 (2010).

[18] A. Fernandez-Pacheco, J. Orna, J. M. D. Teresa, P. A. Algarabel, L. Morellon, J. A. Pardo, M. R. Ibarra, E. Kampert, and U. Zeitler, Appl. Phys. Lett. **95**, 262108 (2009).

[19] F. Walz, J. Phys.: Condens. Matter. **14**, R285 (2002).

[20] J. García and G. Subías, J. Phys.: Condens. Matter **16**, R145 (2004).

[21] R. Ramos, T. Kikkawa, K. Uchida, H. Adachi, I. Lucas, M. H. Aguirre, P. Algarabel, L. Morellón, S. Maekawa, E. Saitoh, et al., Appl. Phys. Lett. **102**, 072413 (2013).

[22] J. Blasco, M. Sánchez, J. García, J. Stankiewicz, and J. Herrero-Martín, J. Cryst. Growth **310**, 3247 (2008).

[23] J. García, G. Subías, J. Herrero-Martín, J. Blasco, V. Cuartero, M. C. Sánchez, C. Mazzoli, and F. Yakhou, Phys. Rev. Lett. **102**, 176405 (2009).

[24] R. Aragón, D. J. Buttrey, J. P. Shepherd, and J. M. Honig, Phys. Rev. B **31**, 430 (1985).

[25] G. Subías, J. García, J. Blasco, J. Herrero-Martín, M. C. Sánchez, J. Orna, and L. Morellón, J. Synchrotron Radiat. **19**, 159 (2012).

[26] J. Blasco, J. García, and G. Subías, Phys. Rev. B **83**, 104105 (2011).

[27] D. Kim and J. M. Honig, Phys. Rev. B **49**, 4438 (1994).

[28] R. J. Rasmussen, R. Aragón, and J. M. Honig, J. Appl. Phys. **61**, 4395 (1987).

[29] A. Fernández-Pacheco, J. M. De Teresa, J. Orna, L. Morellón, P. A. Algarabel, J. A. Pardo, and M. R. Ibarra, Phys. Rev. B **77**, 100403 (2008).

[30] D. Venkateshvaran, W. Kaiser, A. Boger, M. Althammer, M. S. R. Rao, S. T. B. Goennenwein, M. Opel, and R. Gross, Phys. Rev. B **78**, 092405 (2008).

[31] S. Todo, K. Siratori, and S. Kimura, J. Phys. Soc. Jpn. **64**, 2118 (1995).

[32] W.-L. Lee, S. Watauchi, V. L. Miller, R. J. Cava, and N. P. Ong, Phys. Rev. Lett. **93**, 226601 (2004).

[33] M. S. Senn, J. P. Wright, and J. P. Attfield, Nature **481**, 173 (2012).

[34] M. Ziese and H. J. Blythe, J. Phys: Condens. Matter **12**, 13 (2000).

[35] Y. Pu, D. Chiba, F. Matsukura, H. Ohno, and J. Shi, Phys. Rev. Lett. **101**, 117208 (2008).

[36] N. Nagaosa, J. Sinova, S. Onoda, A. H. MacDonald, and N. P. Ong, Rev. Mod. Phys. **82**, 1539 (2010).

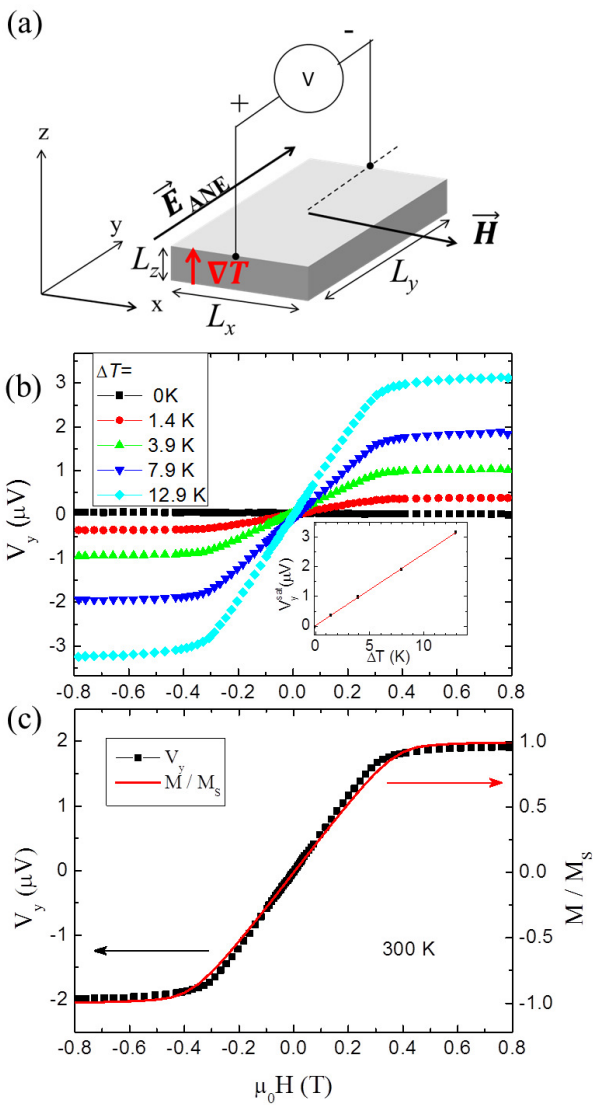

FIG. 1. (Color online) (a) Schematic illustration of the measurement geometry. (b) Results obtained for different applied thermal gradients at 300 K. The inset shows the dependence of V_y^{sat} measured at different magnitudes of the temperature difference (ΔT) across the sample. (c) Comparison of the measured anomalous Nernst voltage and the magnetization of the sample.

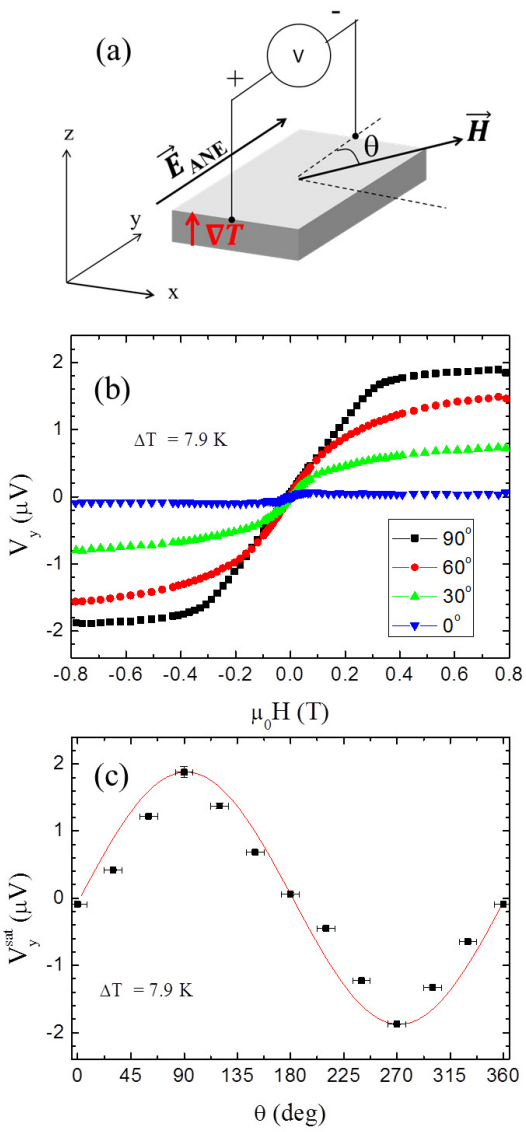

FIG. 2. (Color online) (a) Schematic illustration of the experimental geometry. (b) Dependence of V_y with the direction of applied magnetic field. (c) Angular dependence of the V_y voltage measured at saturation (V_y^{sat}), the solid line corresponds to the best fit to a sinusoidal dependence.

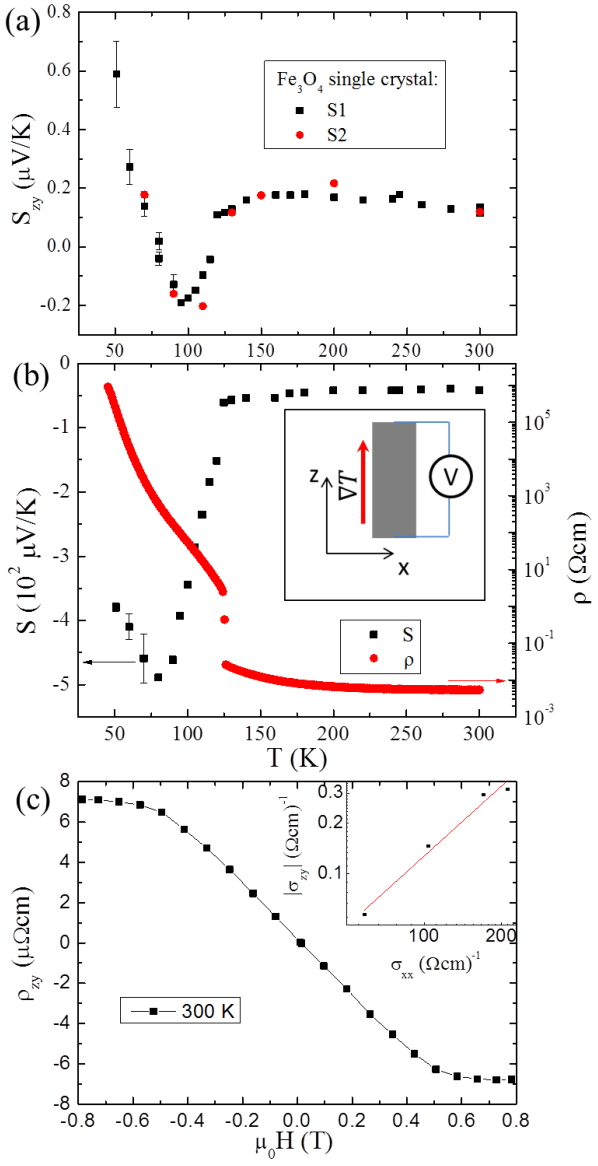

FIG. 3. (Color online) (a) Temperature dependence of the observed anomalous Nernst effect measured for two Fe_3O_4 samples. (b) Seebeck effect and resistivity data. The inset shows the schematic of the Seebeck measurement. (c) Anomalous Hall effect measured at 300 K and fitting to the universal power factor $|\sigma_{zy}| \approx 10^{-4}\sigma_{zz}^{1.6}$ (see inset).

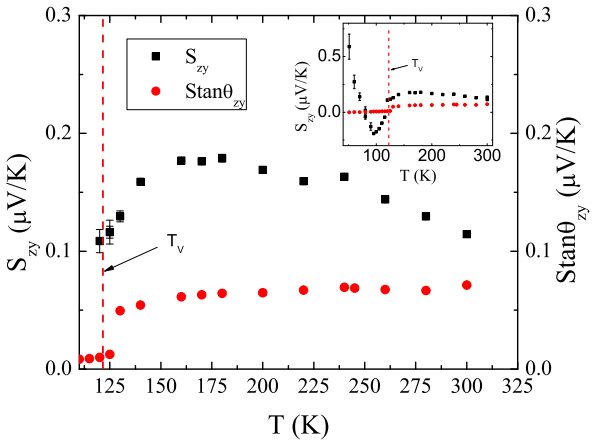

FIG. 4. (Color online) Comparison of the measured anomalous Nernst signal and the joint contribution of the Seebeck component and the AHE above 110 K (inset shows full temperature range).

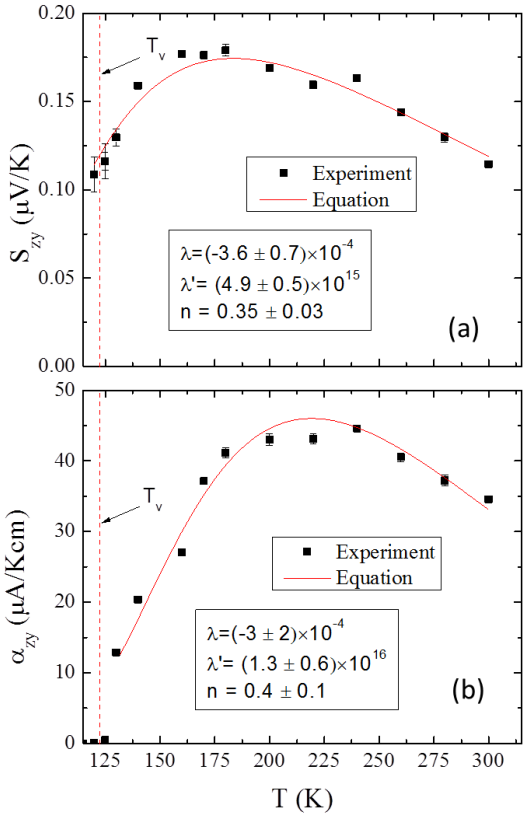

FIG. 5. (Color online) Temperature dependence of (a) S_{zy} and (b) α_{zy} for the Fe_3O_4 single crystal (S1) above the Verwey transition, the solid lines are the best fits using equations (4) and (5).